

Improved Tight Binding Parametrization for the Simulation of Stacking Faults in Aluminium

Anders G. Frøseth* and Randi Holmestad

Department of Physics, Norwegian University of Science and Technology (NTNU), N-7491 Trondheim, Norway

Peter M. Derlet

Paul Scherrer Institute, CH-5232 Villigen PSI, Switzerland

Knut Marthinsen

Department of Materials Technology, Norwegian University of Science and Technology (NTNU), N-7491 Trondheim, Norway

(Dated: January 6, 2021)

We refit the NRL tight binding parameterization for Aluminium by Mehl *et al* [Phys. Rev. B, 61, 4894 (2000)], to a database generated via full potential Linearized Augmented Plane Wave (LAPW) Density Functional Theory (DFT) calculations. This is performed using a global optimization algorithm paying particular attention to reproducing the correct order of the angular symmetries of the tight binding fcc and bcc bandstructure. The resulting parameterization is found to better predict the hcp phase and both the stable and unstable planar stacking fault defect energies.

The empirical tight binding technique can be seen as a compromise between the very accurate but computationally expensive *ab initio* Density Functional Theory (DFT) methods, and the fast but less accurate empirical potential methods such as the Embedded Atom Method (EAM). Although great reductions in computational cost has been achieved for *ab initio* methods by employing a minimal basis set and efficient algorithms that scale linearly with atom number¹, fully self-consistent calculations are still relatively slow for “large” scale Molecular Dynamics (MD) simulations. For empirical tight binding methods, a range of linear scaling techniques have also been developed² and the development of accurate tight binding parameterizations is of utmost importance, if this method is to remain competitive. Furthermore, the strength of the tight binding method, contrary to many EAM parameterizations, is its ability to accurately predict a range of structural properties not included in the fitting database.

The NRL tight binding formalism is a total energy tight binding method based on the fitting of bandstructure eigenvalues and total energies from *ab initio* calculations. One of the advantages of this method is that one is able to fit to the bandstructure and total energy of a given structure simultaneously by redefining the energy zero of the sum of eigenvalues. From DFT, the total energy can be expressed as the sum of the single electron eigenvalues plus an ionic-like term

$$E(n(\mathbf{r})) = \sum_i f(\mu - \epsilon_i)\epsilon_i + F(n(\mathbf{r})) \quad (1)$$

where $f(x)$ is the Fermi function, ϵ_i the electronic eigenvalues, μ the chemical potential, and $F(n(\mathbf{r}))$ the so-called “correction term”^{3,4}. Following Mehl *et al* this can be reformulated by shifting the energy zero of the bandstructure term by a value exactly canceling the “cor-

rection term”:

$$E(n(\mathbf{r})) = \sum_i f(\mu' - \epsilon'_i)\epsilon'_i \quad (2)$$

This shift is taken into account by making the onsite terms environmentally dependent. Using a nonorthogonal two-center Slater-Koster formulation⁵, the tight binding model is then parameterized by fitting the bandstructure and total energies as a function of lattice constant and crystal structure of the tight binding model to a database produced by *ab initio* calculations. The philosophy of the NRL formalism is to include only a handful of high symmetry structures in the fitting database. This method has proven to be successful for a wide range of elements. Further details can be found in Refs.^{3,6}.

We have refitted a tight binding parameterization by Mehl *et al*⁷ for Aluminium using an s , p and d orbital basis, to the full potential LAPW DFT calculations of WIEN2k⁸. As an alternative to the conventional least squares procedure we have used Adaptive Simulated Annealing (ASA), a stochastic global optimization algorithm^{9,10}. Assuming a probability density of states $g_T(\mathbf{x})$ for the parameters space $\{x_i\}$, and a cost function defined by the “energy” $E(x)$. At any step, k , the “probability” for accepting the new cost function E_{k+1} is given by:

$$h(\Delta E) = \begin{cases} \exp(-\Delta E/T) & \text{for } \Delta E > 0, \\ 1 & \text{for } \Delta E < 0. \end{cases} \quad (3)$$

where the parameter $T = T(k)$ defines the “annealing schedule”. For such a system the principle of detailed balance holds, which means that, in theory, all states of the system will be sampled by the algorithm and a global minimum can be found. A weakness of the simulated annealing approach is that it needs to sample a large part of parameter space and can therefore be inherently slow. This is partly remedied in the ASA algorithm by

assuming a probability density for the parameters with “fat” logarithmic tails

$$g_T(x) \equiv \prod_i g_T^i(x_i) = \prod_i \frac{1}{2(|x_i| + T_i) \ln(1 + T_i)} \quad (4)$$

where $x = \{x_i \in [-1, 1]; i = 1, N\}$ is the normalized parameter set. This allows for a very fast annealing schedule

$$T_i(k) = T_{i0} \exp -c_i k^{1/N} \quad (5)$$

in contrast to the conventional linearly decreasing annealing schedule. T_{i0} and c_i are free parameters, which allows the algorithm to adapt to a changing “environment” for the cost functions as the search proceeds. Further details can be found in ref. 9.

In the fitting database we included band-structure data as a function of lattice constant for the fcc and bcc crystal structures using irreducible k-point meshes of 146 for fcc and 91 points for bcc. In order to ensure the correct angular character for each eigenvalue and further constrain the Slater-Koster parameters we block-diagonalized the Hamiltonian for a large number of high symmetry points and directions: the Γ , X , L , W points and Λ , Δ , Σ , S , Z directions for the fcc structure, and the Γ , H , P , N points and Λ , Δ , Σ , F , D , G directions for the bcc structure.

For the DFT calculations we used the input parameters: $R_{mt} = 2.5$ Bohr, $R_{mt}K_{max} = 7$ and $G_{max} = 14$ Ry^{1/2}. Here, R_{mt} is the muffin tin radius, K_{max} is the plane wave cut-off and G_{max} is the maximum Fourier component of the electron density. For the exchange-correlation potential we used the Generalized Gradient Approximation (GGA) of Perdew et. al¹¹.

Fig. 1 displays the TB bandstructure for fcc at $a = 7.65$ Bohr compared to FLAPW *ab initio* calculations and the TB parameterization of Mehl *et. al.* In contrast to the previous parametrization, the ordering with respect to angular character of all bands below 1.25 Ry is now correct. This is important, since otherwise the relative contribution to the bandstructure from each atomic orbital in the LCAO-expansion would break the basic symmetry-requirements of the crystal potential¹².

Fig. 2 displays the energies of state for the fcc, hcp and bcc structures as obtained from a second order Birch fit to the data points derived from the present TB model. Also shown are FLAPW *ab initio* data for fcc and bcc. Tab. I compares the elastic constants from the TB parameterization of the present work with the parameterization of Mehl *et al*⁴, *ab initio* DFT calculations using WIEN2k and experimental values. As can be seen, the TB values are in excellent agreement with the *ab initio* and experimental values, where only the bulk modulus is overestimated. This later discrepancy is probably due to more weight being given (in the present fitting process) to bandstructure data than the equation of state total energy data. The hcp data is in effect a prediction of the tight binding parameterization since only the fcc and bcc

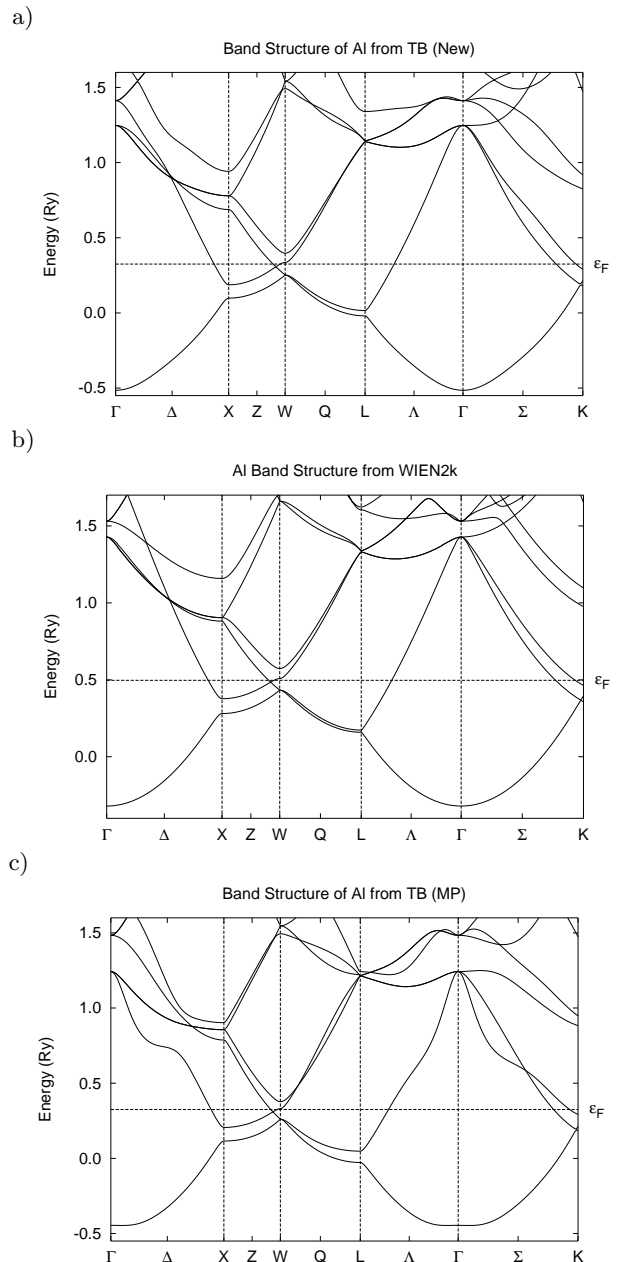


FIG. 1: Band structure for fcc Al at $a = 7.65$ Bohr for a) the new TB parameterization, b) WIEN2k *ab initio* calculations, and c) the TB parameterization of Mehl *et. al.*

structures where fitted. At the obtained equilibrium lattice constants, our fit predicts a fcc-hcp energy difference of 2.1 mRyd per atom, which agrees well with that of the converged (with respect to k-point mesh density using the previously stated *ab initio* parameters) WIEN2k value of 2.0 mRyd. The TB parameterization of Mehl *et. al.* returns a value of 1.8 mRyd.

An important fcc material property for any interatomic model to reproduce is the intrinsic stacking fault surface energy density since it plays a crucial role in the disassociation width of a full dislocation into its constituent

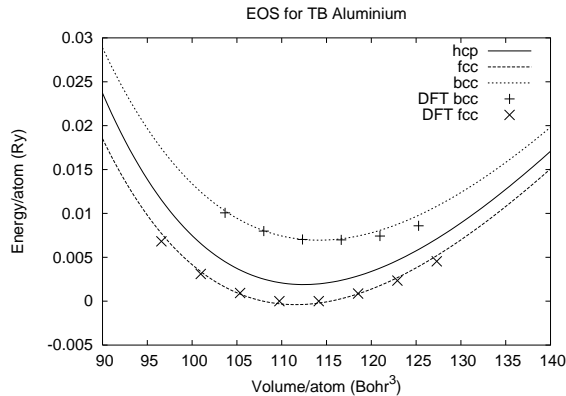


FIG. 2: Energies of state for the bcc, fcc, and hcp phases. Note that only information from bcc and fcc structures was included in the fitting database.

TABLE I: Elastic constants for fcc in units of GPa calculated at $a = 7.65$ Bohr. Experimental results are taken from ref. 13

Property	TB	TB MP	DFT	Exp.
a	7.64	7.58	7.65	7.65
B	92	79	78	79
$C_{11} - C_{12}$	48	59	50	46
C_{44}	27	23	27	28

Shockley partials and is believed to play a role in the issue of why in some cases only partial dislocations are observed in atomistic modeling of the mechanical properties of nanocrystalline materials^{14,15}. An unrelaxed stacking fault is modeled by stacking layers of closed packed planes in the [111] direction using a particular stacking sequence. We choose the primitive vectors of the unit cell to be:

$$\begin{aligned}
 \mathbf{a}_1 &= \frac{1}{2}a\mathbf{y} + \frac{1}{2}a\mathbf{z} \\
 \mathbf{a}_2 &= \frac{1}{2}a\mathbf{x} + \frac{1}{2}a\mathbf{z} \\
 \mathbf{a}_3 &= (4 + \frac{q}{6})a\mathbf{x} + (4 + \frac{q}{6})a\mathbf{y} - (4 - \frac{q}{3})a\mathbf{z}
 \end{aligned} \tag{6}$$

where a is the lattice constant. q is a variable controlling the slip in the [112] direction. This is equivalent to a supercell of 12 close-packed planes, with a variable slip at the 12th layer due to the periodic boundary conditions. For a $q = 0$ we get a perfect fcc crystal represented by the stacking sequence $ABCABC$, and for $q = 1$ we get the full stacking fault $ABC|BC$, where the stacking sequence at the interface corresponds to two 111 planes in which the atoms are hcp coordinated. A mapping of the structural energy for all values of q from 0 to 1 is called a *Bain Path* (or also a generalized stacking fault curve) where an intrinsic stacking fault occurs at $q = 1$. Fig. 3 shows the stacking fault energy as a function of the slip variable, q relative to the fcc energy at $q = 0$. The maximum of the curve defines the unstable stacking

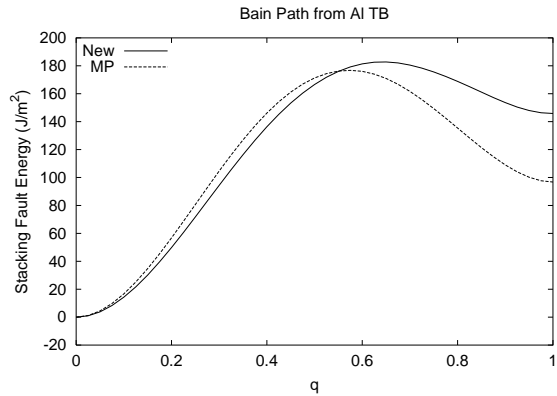


FIG. 3: Bain Path at $a = 7.65$ Bohr comparing the new parameterization with that of Mehl et. al (MP).

fault configuration, which in fig. 3 is near $q = 0.6$.

Table II presents the calculated values for the intrinsic stacking fault energy, γ_{is} , unstable stacking fault energy, γ_{us} , and the ratio γ_{is}/γ_{us} , compared to the TB parameterization of Mehl et. al¹⁶. In addition we include published results from DFT and EAM calculations, and experimental values. The experimentally derived values for γ_{is} vary from a low value of 110 mJ/m² to a high value of 280 mJ/m². However, *ab initio* DFT calculations have consistently shown results in the range 161-166 mJ/m². The EAM potential of Voter and Chen shows values for the stacking fault energies that are seriously underestimated. The important point here is that these values were not included in the fitting database for this potential¹⁷. Similar results have been produced by the EAM potential of Ercolessi and Adams, which has been used in large scale Molecular Dynamics (MD) simulations of extended dislocations¹⁴. In contrast to this, the recently published EAM potential of Mishin and Farkas, show values for the intrinsic and unstable stacking fault energies which are more in line with the *ab initio* calculations. The reason for this is that a value for the intrinsic stacking fault energy was included in the fitting database¹⁸. The TB parameterization of the present work shows a marked improvement over the older parameterization of Mehl *et al* Especially the intrinsic stacking fault energy, γ_{is} , with a value of 146 mJ/m² which is in much better agreement with *ab initio* calculations than a value of 97 mJ/m² of the original fit. Another important improvement is the value of the ratio γ_{us}/γ_{is} , which is a measure of the relative cost of dislocation nucleation with respect to the intrinsic stacking fault energy. For the new TB parameterization this value is 1.3 which is in good agreement with the value of 1.4 from *ab initio* calculations.

The improved prediction of the stacking fault energies is consistent with the corresponding improvement of the hcp cohesive energy and lattice constant of the present model. At the nearest neighbor bond length, the local fcc and hcp environments differ only with respect to their di-

TABLE II: Unstable and intrinsic stacking fault energies for Aluminium in mJ/m²

Property	TB	TB	<i>ab initio</i>	EAM	EAM	Exp. ^e
	Present work	Mehl <i>et al</i> ^a	DFT ^b	Mishin and Farkas ^c	Voter and Chen ^d	
γ_{us}	183	177	224	167	93	–
γ_{is}	146	97	166	146	76	110-216
γ_{us}/γ_{is}	1.3	1.8	1.4	1.2	1.2	–

^aUsing the parameters of ref. 16

^bRef. 19

^cRef. 18

^dRef. 17

^eHigh value from ref. 20, low value ref. 21

hedral angle arrangements. In terms of energy and lattice constant this difference should be sensitive to the angular character of, particularly, the π and δ bonds of the p and d states, and it is precisely such bonding elements that the current parameter-set more accurately reproduces at and near the Fermi level.

In conclusion, we have refitted the tight binding parameters of Mehl *et al* for Aluminium to *ab initio* FLAPW eigenvalues. We have used a stochastic global optimization algorithm and an extended database of high symmetry eigenvalues. As a result we obtain a parame-

terization with an improved representation of the angular symmetries for the Slater Koster parameters. As a consequence we obtain improved predictions for the stacking fault energies without including this information explicitly in the fitting database.

Parts of this work has been supported by the Norwegian Research Council through CPU time on the NOTUR Origin 3800. The static tight-binding code was provided by M. J. Mehl of the Naval Research Laboratory under the U.S. Department of Defense CHSSI program.

* Email: Anders.Froseth@phys.ntnu.no

¹ J. M. Solér, E. Artacho, J. D. Gale, A. Garcia, J. Junquera, P. Orejón, and D. Sánchez-Portal, *J. Phys.: Condens. Matter* **14**, 2745 (2001).

² D. R. Bowler, M. Aoki, C. M. Coringe, A. P. Horsfield, and D. G. Pettifor, *Modelling Simul. Mater. Sci. Eng.* **5**, 199 (1997).

³ M. J. Mehl and D. A. Papaconstantopoulos, *Phys. Rev. B* **54**, 4519 (1996).

⁴ M. J. M. Sang H Yang and D. A. Papaconstantopoulos, *Phys. Rev. B* **57**, R2013 (1998).

⁵ J. C. Slater and G. F. Koster, *Phys. Rev.* **94**, 1498 (1954).

⁶ M. J. Mehl and D. A. Papaconstantopoulos, *Topics in Computational Materials Science* (World Scientific, Singapore, 1998), chap. V, pp. 169–213.

⁷ M. J. Mehl, D. A. Papaconstantopoulos, N. Kioussis, and M. Herbranson, *Phys. Rev. B* **61**, 4894 (2000).

⁸ P. Blaha, K. Schwarz, G. Madsen, D. Kvasnicka, and J. Luitz, WIEN2k, *An Augmented Plane Wave + Local Orbitals Program for Calculating Crystal Properties* (Karlheinz Schwarz, Techn. Universitat Wien, Austria, 1999), ISBN 3-9501031-1-2.

⁹ A. G. Frøseth, P. Derlet, and R. Høier, in *Combinatorial and Artificial Intelligence Methods in Materials Science*, edited by I. Takeuchi, H. Koinuma, E. J. Amis, J. M. Newsam, and L. T. Wille, MRS Symposium Proceedings vol. 700 (Materials Research Society, 2001).

¹⁰ L. Ingber, *Adaptive Simulated Annealing (ASA)*, *Global*

Optimization C-code (Caltech Alumni Association, CA, 1993).

¹¹ J. P. Perdew, S. Burke, and M. Ernzerhof, *Phys. Rev. Lett.* **77**, 3865 (1996).

¹² T. Inui, Y. Tanabe, and Y. Onodera, *Group Theory and Its Applications in Physics* (Springer-Verlag, Berlin Heidelberg New York, 1995), 2nd ed.

¹³ G. Simmons and H. Wang, *Single Crystal Electric Constants and Calculated Aggregate Properties: A Handbook* (MIT Press, Cambridge MA, 1971).

¹⁴ V. Yamakov, D. Wolf, M. Salazar, S. R. Phillpot, and H. Gleitzer, *Acta Mater.* **49**, 2713 (2001).

¹⁵ H. V. Swygenhoven, P. M. Derlet, and A. Hasnaoui, *Phys. Rev. B* **66**, 024101 (2002).

¹⁶ M. J. Mehl, D. A. Papaconstantopolous, N. Kioussis, and M. Herbranson, *Phys. Rev. B* **61**, 4894 (2000).

¹⁷ A. F. Voter and S. P. Chen, in *High temperature ordered intermetallic alloys*, edited by R. W. Siegel, J. R. Weertman, and R. Sundan, MRS Symposium Proceedings vol. 82 (Materials Research Society, Pittspurgh, 1987).

¹⁸ Y. Mishin, D. Farkas, M. J. Mehl, and D. A. Papaconstantopolous, *Phys. Rev. B* **59**, 3393 (1999).

¹⁹ G. Lu, N. Kioussis, V. V. Butalov, and E. Kaxiras, *Phys. Rev. B* **62**, 3099 (2000).

²⁰ J. P. Hirth and J. Lothe, *Theory of Dislocations* (Wiley, New York, 1992), 2nd ed.

²¹ V. Vitek, *Prog. Mater. Sci.* **36**, 1 (1992).